INTERACTIVE CLOUD AND RADIATION IN THE METEOROLOGICAL OFFICE GENERAL CIRCULATION MODEL

Julia M Slingo

Dynamical Climatology Branch, Meteorological Office,

Bracknell, England

1. INTRODUCTION

In the past few years interactive radiation schemes have been developed for the 5-level and 11-level general circulation models used in the Dynamical Climatology Branch of the Meteorological Office. Both schemes are similar in design, the main differences arising from the models' differing vertical resolutions. The schemes have been used extensively in general circulation studies usually with the constraint of fixed climatological zonal mean cloud amounts.

The original motivation for the development of interactive radiation in the 11-level model was the possibility of using GATE data to derive a cloud parametrization scheme. The development of this cloud prediction scheme is described in detail in Slingo (1980a) and similar methods have been used to extend the scheme to the whole globe using FGGE data (Wilderspin 1980). So far studies of interactive cloud in the 11-level model have been confined to short period integrations. The main effort has been with the limited area tropical model in which the effect of interactive clouds on circulation and rainfall during a 3-day forecast has been studied in some detail. These results, with particular emphasis on the effect on convective activity, were described at the ECMWF Workshop on 'The parameterization of cumulus convection' (Slingo 1978). This paper will therefore deal only with the cloud and radiation schemes developed for the 5-level model which is used primarily for longer period integrations.

One of the main concerns of the Dynamical Climatology Branch is the provision of a general circulation model suitable for climate change experiments. An essential part of this is the development of an interactive radiation scheme since schemes based on climatology (e.g. Corby et al, 1977), although computationally economical, have several drawbacks. Firstly they assume the specific humidities and cloud amounts to be fixed in time and are thus unsatisfactory for simulating a climate substantially different from that for which the assumed humidities and clouds are valid. Secondly, climatological schemes are unsuitable for assessing the effects of environmental changes, whether natural or man-made, since they are unable to respond to changes in the humidity and cloud distributions caused by changes in the circulation patterns.

The interactive radiation and cloud schemes for the 5-level model have been designed with climate change studies very much in mind. For example, it is important for long period integrations that the global mean radiation budget is accurately simulated and that the radiative flux at the surface is adequately represented, particularly if an interactive ocean model is to be incorporated. For short period integrations such factors are of lesser importance. Consequently it is desirable not only that cloud is predicted in the correct geographical

locations but also that the overall effect of clouds on the whole globe is correctly simulated. Thus it is importance that the radiation scheme accurately represents the earth/atmosphere radiation budget when applied to present day conditions before it can be used with any confidence in climate change experiments.

Much of the work done to date with the 5-level model radiation scheme has been designed to ensure that the simulated radiation budget compares favourably with that observed by satellites when the constraint of seasonally varying climatological cloud amounts is applied. Some results of this work will be shown in this paper but are discussed in more detail in Slingo (1980b). In recent months a cloud parameterization scheme has been developed for the 5-level model using the same approach as that adopted in the scheme derived from GATE data (Slingo 1980a). The scheme has been tested in a 50-day integration from which preliminary results will be presented.

2. TREATMENT OF CLOUD AND RADIATION IN THE 5-LEVEL GENERAL CIRCULATION MODEL

The model is similar to that described by Corby et al (1977) except that the representations of radiation and surface exchange processes have been changed and the moist gas constant is used. In the vertical, the model uses a σ - coordinate system (σ = pressure/surface pressure) with the atmosphere divided into five layers of equal mass. The horizontal grid gives a quasi-uniform resolution over the sphere with a grid length of approximately 330 km.

(a) Description of the radiation scheme

For the calculation of radiative fluxes, the atmosphere is divided into ten equal layers with temperatures and humidities interpolated from the five model levels. Not only does this allow a better representation of the temperature and humidity gradients but also a greater freedom of choice for cloud top heights which, for computational speed, are placed at layer boundaries. The scheme allows for four cloud types - low, medium, high and convective - which can be of varying heights and thicknesses. Cloud overlap is assumed to be random. With the exception of convective cloud, cloud thickness is not restricted to an intergral number of layers but is allowed to take any value. This avoids, for example, unrealistically thick cirrus cloud and allows a better specification of the cloud base temperature which is important for determining the surface infrared flux and also the net flux divergence across a cloud layer. The cloud base temperature is calculated from the cloud top temperature by assuming a moist adiabatic lapse rate in the cloud. In addition both low and convective cloud can, when appropriate, be associated with the boundary layer top which is

defined explicitly in the model.

The radiation scheme is similar in approach to that described by Manabe and Strickler (1964). Solar radiation is absorbed and scattered by atmospheric gases and clouds and by the earth's surface. The absorptions by ozone, carbon dioxide and water vapour are determined as a function of the effective optical thickness. No temperature dependence is included and both ozone and carbon dioxide absorptivities are assumed independent of pressure for solar wavelengths. The solar absorptivity curves for ozone and water vapour have been taken from Manabe and Möller (1961); the curve for carbon dioxide was derived from the empirical fits for the absorption bands given by Roach (1961). The gases are assumed to absorb radiation independently of one another. Monthly zonal mean values of the ozone optical thickness have been evaluated from the data of Dopplick (1970) and London et al (1976) and are used to calculate the total absorption by ozone for the top model layer, $\sigma = 0.0 - 0.2$. The annual variation in the solar constant due to the eccentricity of the earth's orbit has been incorporated in the scheme. For reasons of computational economy the radiation scheme is called every few hours rather than every time-step so that a mean cosine of the zenith angle is calculated for each point in order to obtain an accurate estimate of the incoming solar radiation over this period. Rayleigh scattering is allowed for implicity by reducing the incoming solar radiation by 3%.

The surface albedos used in the model are given in Table 1. Over land they are a function of latitude and the snow depth predicted by the model, thus incorporating the snow-albedo feedback. The increased absorption at the surface as a result of multiple reflections between clouds and the ground has also been included. At present the cloud radiative properties are fixed at the values shown in Table 2 although the scheme has been designed to allow a variation in these parameters if desired.

The treatment of infrared radiation is based on the emissivity or 'grey body' approximation. The scheme treats the absorption and emission by the bands of water vapour and carbon dioxide and by the water vapour continuum. Since the model does not resolve the stratospheric temperature structure, the effect of the 9.6 μm band of ozone has been included by adding a zonal mean heating rate, derived from Dopplick (1970), to the heating rate for the top model layer. This is updated monthly as are the ozone path-lengths used in the solar flux calculations. Overlapping of the bands of water vapour and carbon dioxide and of the water vapour continuum is allowed

Table 1: Surface albedos used in the radiation scheme

Surface Type	Albedo	Remarks
Sea	0.06	
Land (snow-free)	0.146 - 0.225	Varies with latitude (Corby et al 1977)
Snow-covered land	$\alpha_L + 0.12\sqrt{\text{Snowdepth}}$	α_L = snow-free land albedo. Upper limit of 0.6 on albedo. Snowdepth in mm water equivalent.
Sea-ice and permanent snow cover	0.8 for $T_* < 271.2$ 0.5 for $T_* \geq 271.2$	T_* is surface temperature (K)

Table 2: Cloud properties used in the radiation scheme

Cloud Type:-	Low	Medium	High	Convective
Thickness ($\Delta\sigma$; $\sigma = P/P_*$)	0.05	0.05	0.02	Variable
Reflectivity	0.7	0.6	0.2	0.7
Transmissivity	0.2	0.3	0.75	0.2
Absorptivity	0.1	0.1	0.05	0.1
Emissivity	1.0	1.0	0.5	1.0

Table 3: Division of the longwave spectrum demonstrating the regions of overlap

Spectral region (cm^{-1})	0-500	500-700	700-800	800-1200	1200-2850
Water vapour bands	X	X	X	X	X
Water vapour continuum			X	X	
Carbon dioxide		X	X		

X - Gas included in this region.

for by dividing the infrared spectrum into four regions as shown in Table 3. The emissivities and absorptivities of the individual gases for these spectral divisions were calculated using a scheme based upon the Mayer-Goody random band model (Hunt and Mattingly 1976) with spectroscopic data from McClatchey et al (1973). With the exception of high cloud which has an emissivity of 50%, all clouds are treated as black bodies. All fluxes are calculated at model layer boundaries and the heating rate for that layer calculated using flux differencing.

(b) The performance of the radiation scheme

The performance of the radiation scheme has been assessed in an extended integration covering several annual cycles. The model uses seasonally varying climatological sea surface temperatures, incoming solar radiation and zonal mean climatological cloud amounts. This means that the model has been constrained so that it does not deviate far from the observed seasonal cycle. The ability of the radiation scheme to simulate the earth's radiation budget can then be assessed by comparing the model results with observed budgets from satellites. As mentioned earlier the 5-level model is designed for climate change experiments so that considerable emphasis is placed on a realistic simulation of the total radiation budget. The use of climatological sea surface temperatures and cloud amounts has certain advantages in that it allows a study of present day climatology to be made using model results in which data on many aspects of the general circulation are available on a global scale. For example the model results have been used to assess the importance of clouds and the earth's surface in determining the global radiation budget. These results will be presented briefly here but are discussed in more detail in Slingo (1980b).

The seasonal variations of the global mean components of the model's radiation budget are shown in Fig. 1 and have been compared with those given by Ellis and Vonder Haar (1976), Gruber (1978) and Jacobowitz et al (1979). Although the model's planetary albedo (Fig. 1(b)) is generally higher than the observed values, the seasonal variation is similar to the observed, the maximum and minimum albedos occurring in the northern hemisphere winter and summer, respectively. In addition the model has a secondary maximum in May which is also evident in the data of Ellis and Vonder Haar and Jacobowitz et al. The seasonal variation of the total solar absorption follows that of the incoming solar radiation to a large extent with slight modifications - notably a reduction in amplitude - due to the seasonal changes in planetary albedo. The outgoing radiance given by the model has a variation similar to that of the observed data of Gruber and Jacobowitz et al. (The sharp

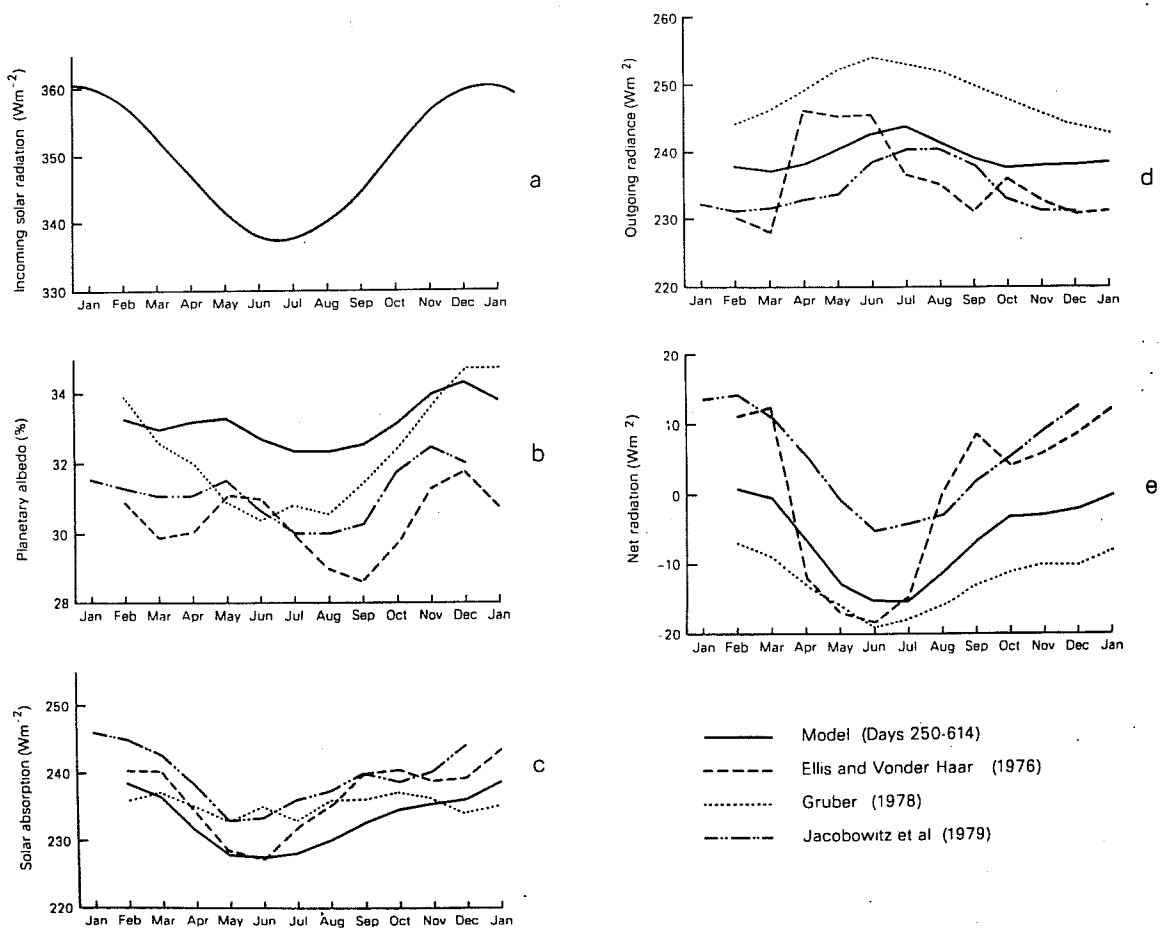

Fig. 1 Seasonal variation of the components of the global mean radiation budget derived from satellite observations and from the model. (a) Incoming solar radiation, (b) Planetary albedo, (c) Solar absorption, (d) Outgoing radiance, (e) Net radiation.

rise and fall from March to April and from June to July in the data of Ellis and Vonder Haar is probably associated with a change in satellites during those months). In general the maximum outgoing radiance occurs in the northern hemisphere summer although the observations differ as to its exact timing. The combination of a minimum in total solar absorption and a maximum in outgoing radiance during the northern hemisphere summer gives a pronounced minimum in the net radiation in June and July. The model's maximum net radiation occurs in January and February, again in agreement with the observations. If the global annual average of the net radiation ($-6 Wm^{-2}$) were removed from the annual cycle, the model earth-atmosphere system would show a surplus from October through to March and a deficit from April through to September.

As well as comparing global mean results, the latitudinal distribution of the various components of the earth's radiation has also been studied (Slingo 1980b). Time-latitude diagrams of planetary albedo and outgoing radiance have been compiled and have been compared with similar diagrams based on data from NOAA satellites (Gruber 1978). These show that the planetary albedo simulated by the model shows reasonable agreement with the observed distribution. The seasonal variation produced by the model is good in middle latitudes of the northern hemisphere, but is less satisfactory in the southern hemisphere where the model's neglect of the variation of sea surface albedo with solar zenith angle may be important. In the tropics the positions of the maxima and minima, associated with the seasonal shift of the ITCZ, are represented fairly well in the model although the magnitude of these variations is under-estimated, more especially south of the equator. The model's outgoing radiance, which with the planetary albedo, determines the net radiation budget, shows a similar seasonal variation to the observed values. The latitudinal and seasonal variations in the tropics are qualitatively realistic but, as with the planetary albedo, the range is less than the observed.

As was seen in Fig. 1, both the planetary albedo and the outgoing radiance display variations which are not related to these in the incident solar radiation. It seems that many of the features of the annual cycle of the global mean radiation budget can be associated with the asymmetry in the distribution of land and sea between the two hemispheres (eg. Raschke et al (1973); Jacobowitz et al (1979)). In Figs. 2 and 3 the model's seasonal variations in planetary albedo and outgoing radiance are shown for each hemisphere. Since the model provides detailed information for the whole globe on the variables that determine the components of the radiation

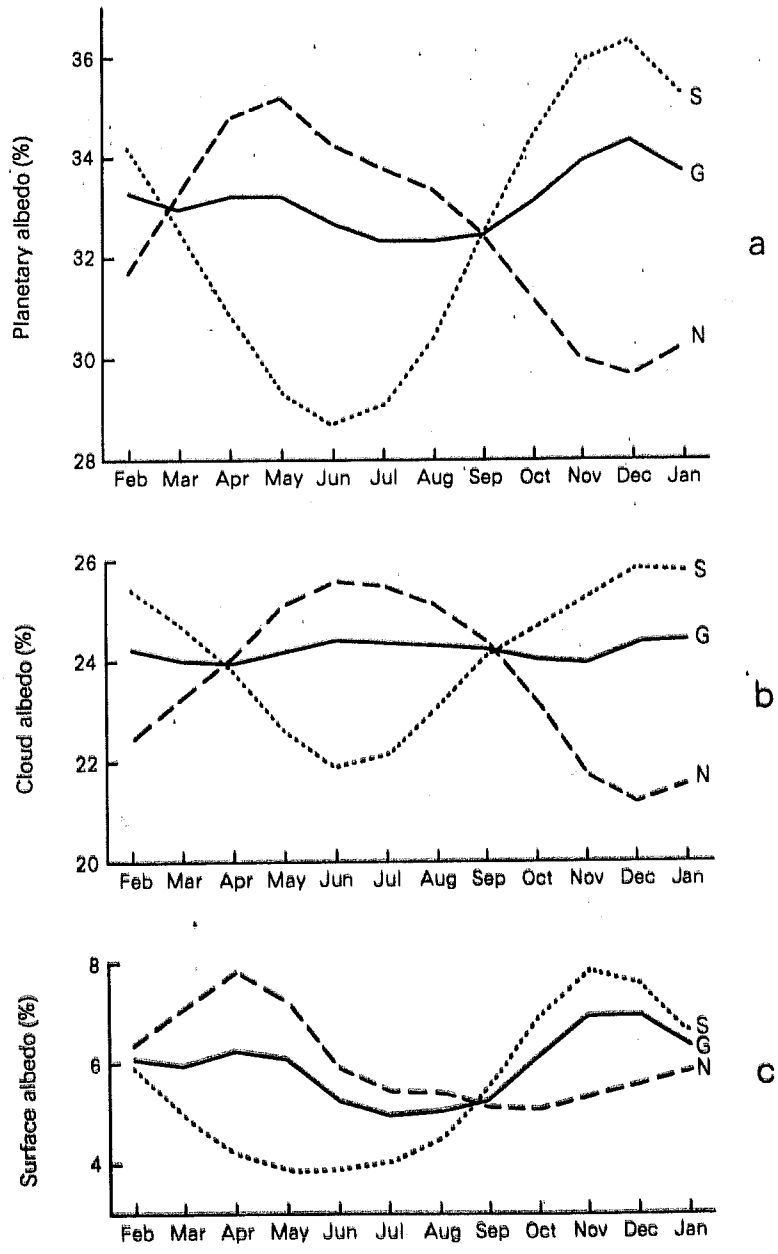

Fig. 2 Seasonal variation of hemispheric and global mean values of (a) planetary albedo, (b) cloud albedo and (c) surface albedo

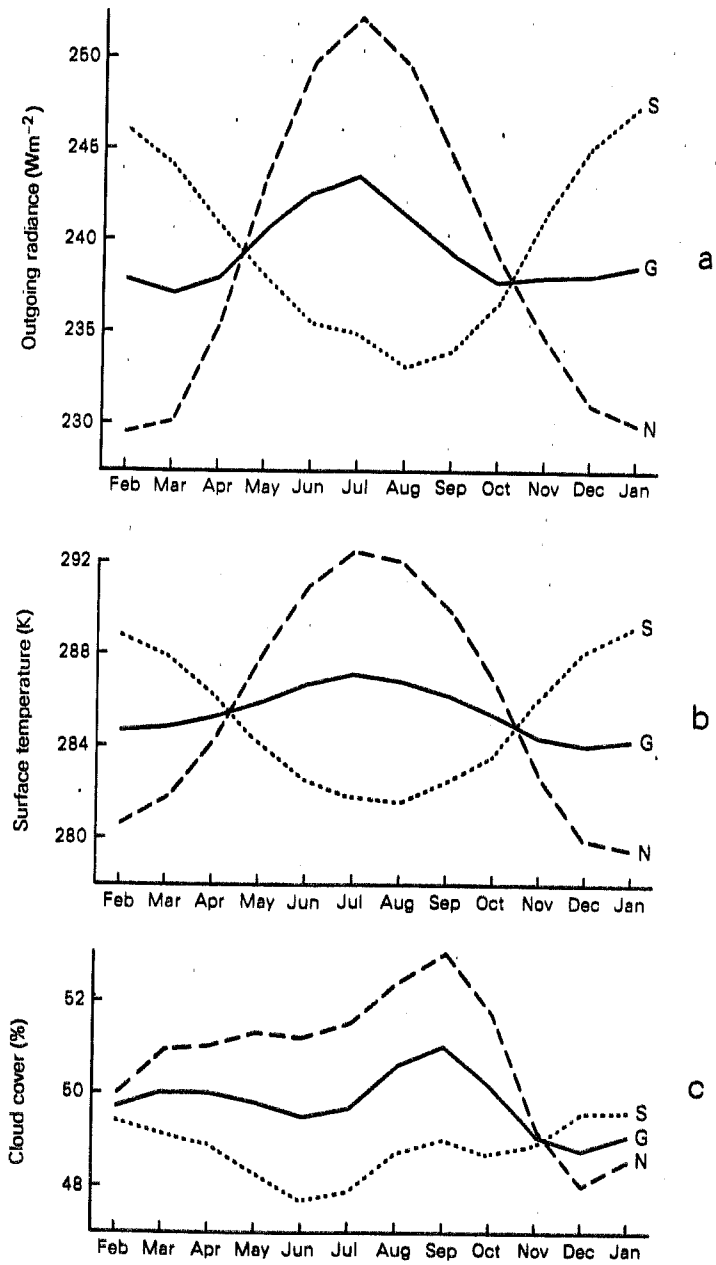

Fig. 3. Seasonal variation of hemispheric and global mean value of (a) outgoing radiance, (b) surface temperature and (c) cloud cover

budget, it is possible to isolate the contributory factors in the seasonal variations produced by the model. The main determinants of the planetary albedo are the surface albedo and the cloud cover. In Fig. 2 the percentages of the incoming solar radiation reflected by clouds and by the surface are shown for each month and for each hemisphere. It is clear from Figs. 2(a) and 2(b) that clouds play an important part in determining the variations in the hemispheric planetary albedos. However the symmetry of the variations in the hemispheric cloud albedos has resulted in a global cloud albedo which varies only slightly with season. Consequently clouds contribute little to the seasonal change in the global planetary albedo (Fig. 2(a)). In contrast the variation in surface albedo is quite different in the two hemispheres (Fig. 2(c)). In the southern hemisphere the maximum and minimum albedos coincide with the solstices due to the variation in illumination of the highly reflecting pole. In the northern hemisphere the maximum and minimum albedos are nearer the equinoxes and can be associated with the seasonal variation in sea-ice and snow-cover. The maximum in the northern hemisphere surface albedo in April (Fig. 2(c)) is a combination of the increasing illumination of the polar regions and the high albedo of the snow-covered continents. As the snow melts in spring and early summer the surface albedo decreases. Similarly the minimum northern hemisphere surface albedo occurs in October; thereafter the spread of snow southwards increases the hemispheric mean surface albedo. It is clear from Fig. 2 that, on a global scale, the seasonal variation in surface albedo dominates that in the planetary albedo.

The seasonal variation in the outgoing radiance is greater in the northern hemisphere than the southern hemisphere (Fig. 3) so that the maximum in the global mean outgoing radiance coincides with that in the northern hemisphere. The dependence of the outgoing radiance on the surface temperature is evident in Fig. 3 where the monthly mean surface temperatures for each hemisphere have been plotted. The extensive oceans of the southern hemisphere are less responsive than the land masses of the northern hemisphere to the annual course of the solar radiation so that the northern hemisphere surface temperatures show a greater difference between winter and summer. Consequently the global mean surface temperature (Fig. 3) has a maximum in the northern hemisphere summer when the incoming solar radiation and total absorption are at their lowest. It is clear from Fig. 3 that the seasonal change in cloudiness has only a small effect on the shape of the outgoing radiance curves and that it is the variation in surface temperature which is the dominant factor. These results agree with those of Cess (1976) based on satellite data and zonal mean climatology.

The dependence of the seasonal variation of the earth's radiation budget on the surface has highlighted the need for a good simulation of sea-ice cover and surface temperature. Other variations in surface albedo, not included in this study, such as those associated with changes in vegetation and solar zenith angle may also be important. It would be misleading, however, to dismiss variations in cloudiness as insignificant in determining the radiation budget. For example, clouds play an important part in determining the variations in the hemispheric planetary albedos (Fig. 2) and on a latitudinal scale, can be related clearly to the variations in planetary albedo and outgoing radiance, particularly in the tropics.

(c) Cloud prediction scheme

Although the model is capable of reproducing a realistic zonal mean radiation budget when climatological cloud amounts are used, satellite data have shown (eg. Figs. 4(a) and (b)) that there are pronounced longitudinal variations which the model would fail to predict. For example there are areas of enhanced planetary albedo associated with the cloudiness of the ITCZ, the sub-tropical stratocumulus fields and the south-west monsoon. Similarly the outgoing radiance is low in areas with high cloud, such as the ITCZ and the south-west monsoon. Cloud-free areas such as the Sahara have high values of outgoing radiance which are not well represented in the model when zonal mean clouds are used. A more realistic geographical distribution of planetary albedo and outgoing radiance could be obtained if clouds were predicted by the model. In that case a better representation of the longitudinal variation in cloudiness might be obtained.

In recent months a cloud prediction scheme has been developed and tested in the 5-level model. Apart from providing a more realistic distribution of radiative heating, it will also allow a study of how a change in cloudiness might feedback on itself through the response of the atmosphere to the resultant change in surface temperature and atmospheric stability. Any reliable estimates of the effects of, for example, increasing CO_2, changes in the composition of the stratosphere, and disposal of waste heat from nuclear reactors require a prediction of cloudiness and its effect on the general circulation.

There are major problems involved in predicting cloudiness in a numerical model. Firstly, the formation and dissipation processes are poorly understood and secondly, most clouds are sub-grid scale, if not horizontally then vertically. The cloud parametrization scheme used in the 5-level model is based on a very simple approach, namely that condensation on the smallest

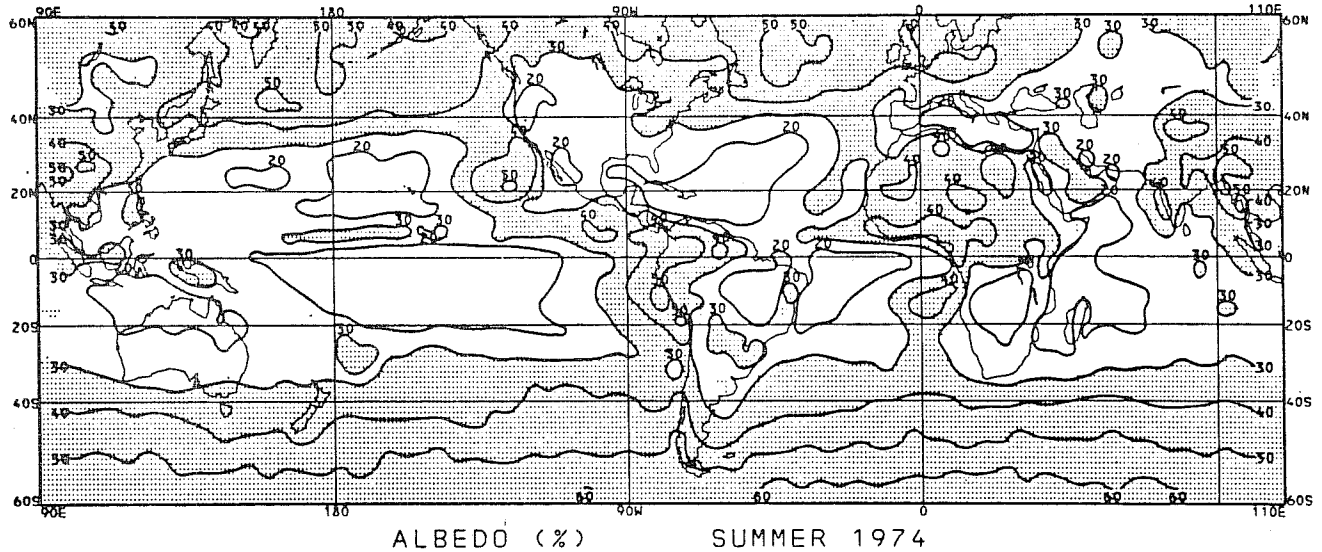

a

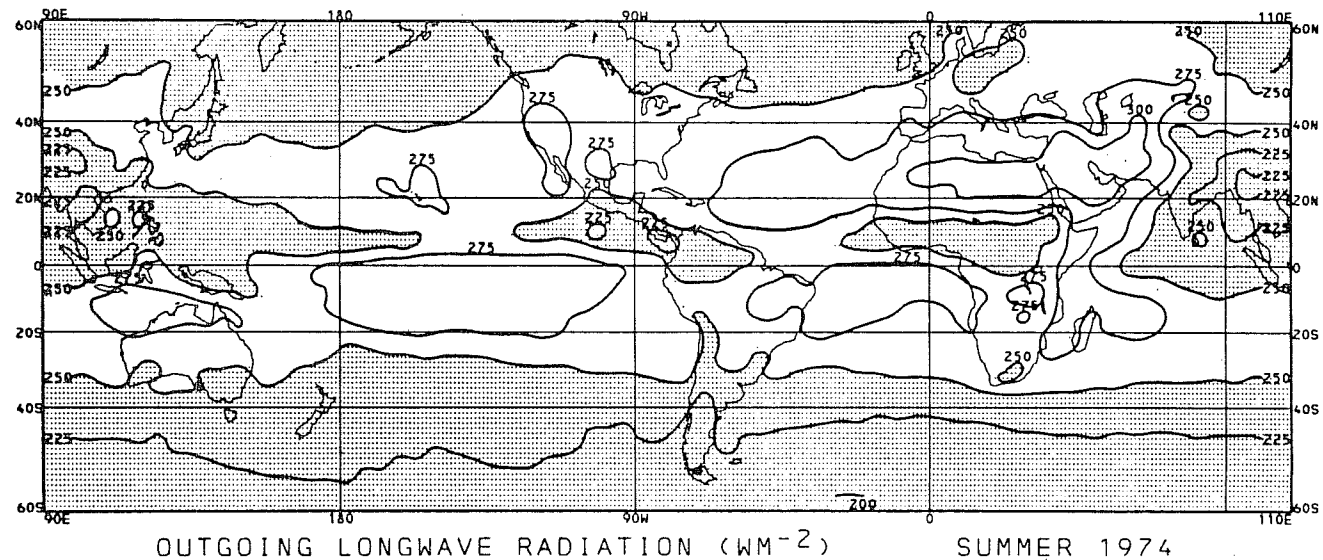

b

Fig. 4 Maps of (a) planetary albedo and (b) outgoing radiance derived from NOAA satellite data (Winston et al 1979)

scales is part of a larger scale condensation regime related to the synoptic scale situation. This method was used originally in the development of the cloud prediction scheme for the 11-layer limited area tropical model which is described in detail in Slingo (1980a). This scheme is not directly transferable to the 5-level model since the predictive equations are dependent on the model's horizontal and vertical resolution. For example, the coarser the horizontal resolution the greater the probability that the grid square will contain some cloud but the lower the probability that it will be completely cloudy. The scheme is also dependent on how realistically the model distributes humidity in the vertical.

In the 5-level model, layer cloud amounts are predicted using quadratic functions of relative humidity with 100% cloud cover occurring with saturation. In addition low layer cloud is also related to the model's temperature structure so that when a lower tropospheric inversion forms (eg. the tradewind inversion), low layer cloud amounts are a function of the strength of the inversion as well as the relative humidity under the inversion. An additional constraint is applied that an unstable layer must exist below the inversion before cloud can form. This avoids the unrealistic formation of cloud in such circumstances as under the polar night inversion or in association with anticyclones (Wilderspin 1980). The predictive equations for layer clouds are as follows, where R is relative humidity (%):-

High cloud, $C_H = 0.00111\ (R - 70)^2$ for $R \geqslant 70$

Medium cloud, $C_M = 0.01\ (R - 90)^2$ for $R \geqslant 90$

Low cloud, C_L:-

(i) In the presence of a lower tropospheric inversion $\Delta\theta/\Delta p \leqslant -0.07$ and an unstable layer below the inversion:-

$$C_L = -16.67\ \Delta\Theta / \Delta p \quad - 1.167 + 0.01\ (R - 90)^2 \text{ for } R \geqslant 90$$

or $$C_L = -16.67\ \Delta\Theta / \Delta p \quad - 1.167 - (90 - R)/180 \text{ for } R < 90$$

where $\Delta\Theta/\Delta p$ is the potential temperature lapse rate between $\sigma = 0.9$ and $\sigma = 0.7$.

(ii) Otherwise (i.e. no inversion or no unstable layer below the inversion)

$$C_L = 0.01\ (R - 90)^2 \quad \text{for} \quad R \geqslant 90$$

Convective cloud amounts are predicted using the convective mass

flux from the model's convection scheme.

So far the scheme has only been tested in a 50-day integration starting from day 918 (equivalent to December 1st) of the annual cycle integration discussed earlier. The radiation and cloud schemes are called every 2 hours of model time, the radiative heating rates and fluxes remaining fixed during that period. The results of this integration have been compared with those from a control integration which used zonal mean climatological cloud amounts derived mainly from the data of Telegadas and London (1954) and Sasamori et al (1972). Further information on Arctic and Antarctic cloudiness was obtained from Huschke (1969) and Phillpot (1968).

A mean of the last 30 days of the integration have shown that the predicted cloud amounts are in good agreement with the climatological amounts used in the control integration. Global mean cloud amounts of 31, 8, 12 and 7% for low, medium, high and convective clouds respectively, were obtained compared with climatological estimates of 32, 8, 16 and 2%. A global total cloud cover of 47.5% was predicted compared with 49% from climatology. The radiation budget for the last 30 days shows a global mean net radiation of $0.8 Wm^{-2}$ associated with a planetary albedo of 32.5% and an outgoing radiance of $242.6 Wm^{-2}$. Equivalent figures for the control integration with fixed cloud are $-1.9 Wm^{-2}$, 34.3% and $238.6 Wm^{-2}$. Thus, in terms of global means, the cloud parametrization scheme appears to be performing satisfactorily.

In Fig. 5 the latitudinal distribution of total cloudiness predicted by the model is compared with the climatological distribution as used in the control integration. The model has successfully reproduced the general shape of the distribution with the main maxima in cloudiness associated with the depression belts. The increase in cloudiness in equatorial regions associated with the ITCZ is also well predicted. However the model has produced too much cloud poleward of 50^{o} particularly in the northern hemisphere and too little cloud in the sub-tropics of the southern hemisphere. One shortcoming of many cloud prediction schemes (eg. GLAS model (Herman 1980)) is their tendency to produce too much cloud over the winter pole. As Fig. 5 shows this has been largely overcome with this scheme by imposing the constraint that an unstable layer must exist above the surface (Wilderspin 1980).

Verification of the geographical distribution of each cloud type is extremely difficult since no global climatology exists. Thus the cloud prediction scheme has been assessed mainly by checking that the cloud

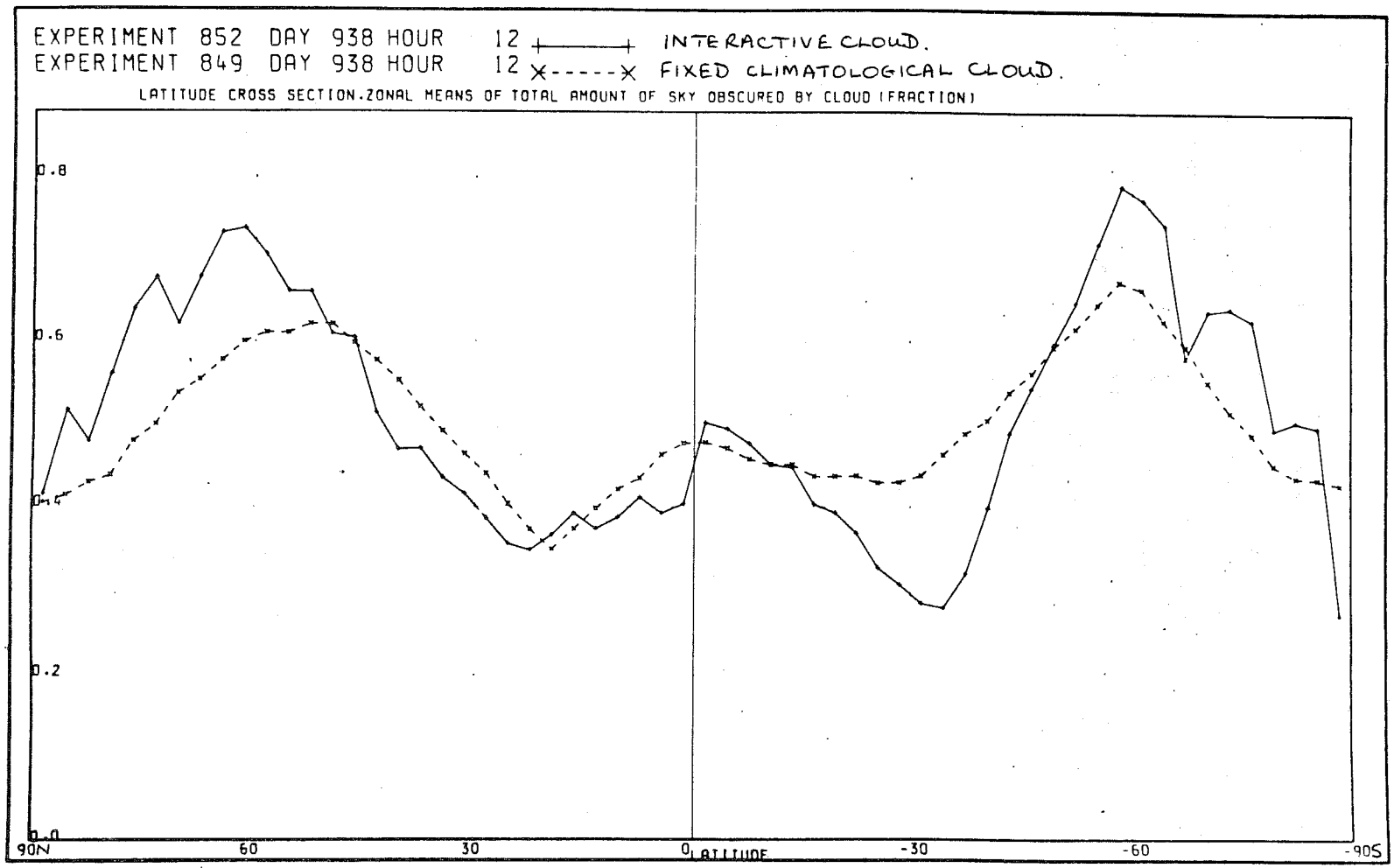

Fig. 5 Comparison of the January zonal mean total cloudiness produced by the interactive cloud scheme with that from climatology

occurs in a synoptically correct location. In the distribution of high cloud (Fig. 6) the ITCZ is clearly visible as are the convectively active regions of SE Asia. However there is a clear tendency for high cloud to form over the mountains which is not supported by observations. (It is possible that this problem may be associated with the use of relative humidities on the model sigma levels rather than at specific pressure levels). The distribution of medium cloud (Fig. 7) also shows a tendency for cloud to form over the mountains. In the tropics medium cloud is associated mainly with the ITCZ in agreement with a study made of surface observations and satellite pictures during GATE (Slingo 1980a). The extensive area of medium cloud over Northern Asia is difficult to verify and is probably unrealistic.

The distribution of low cloud (Fig. 8) shows several features which hitherto have been difficult to predict. For example the scheme has modelled the areas of stratocumulus off the west coasts of South Africa and South America. Failure to predict these layer clouds was a feature of earlier schemes (eg. Hunt 1976; Kasahara and Washington 1971). The cloud-free areas over the Sahara and Australia have been simulated quite well. In extra-tropical latitudes the model has produced the extensive low cloud associated with the depression belt to the north of the Antarctic ice-cap. In the northern hemisphere low layer cloud occurs predominantly along the eastern coasts of the major continents, over Scandinavia and in a zone across central Asia. These results can be compared qualitatively with those from a study of the absolute frequency of occurrence of stratus and cumulus clouds made by Shapovalova (1979) using data from the 'Meteor' satellite over a 4-year period, 1972-1975. Fig. 9, from Shapovalova (1979), shows that stratus clouds occur most frequently over the North Sea and Scandinavia, western Asia and to the east of Asia and North America. Assuming that frequency can be positively correlated with amount then the model has shown some skill in predicting the distribution of low layer cloud.

In Fig. 10 the 30-day mean distribution of convective cloud is shown. As expected from the nature of the cloud, amounts are fairly small. The main areas of convective cloudiness occur in the North Atlantic and North-west Pacific and can be related to the cold fronts associated with the Icelandic and Aleutian lows. Comparison with Fig. 8 shows that, in the North Atlantic especially, the cloud produced by the model is predominantly convective. The ITCZ is not particularly well-defined in the convective cloud cover and the amounts predicted by the model in this region are rather

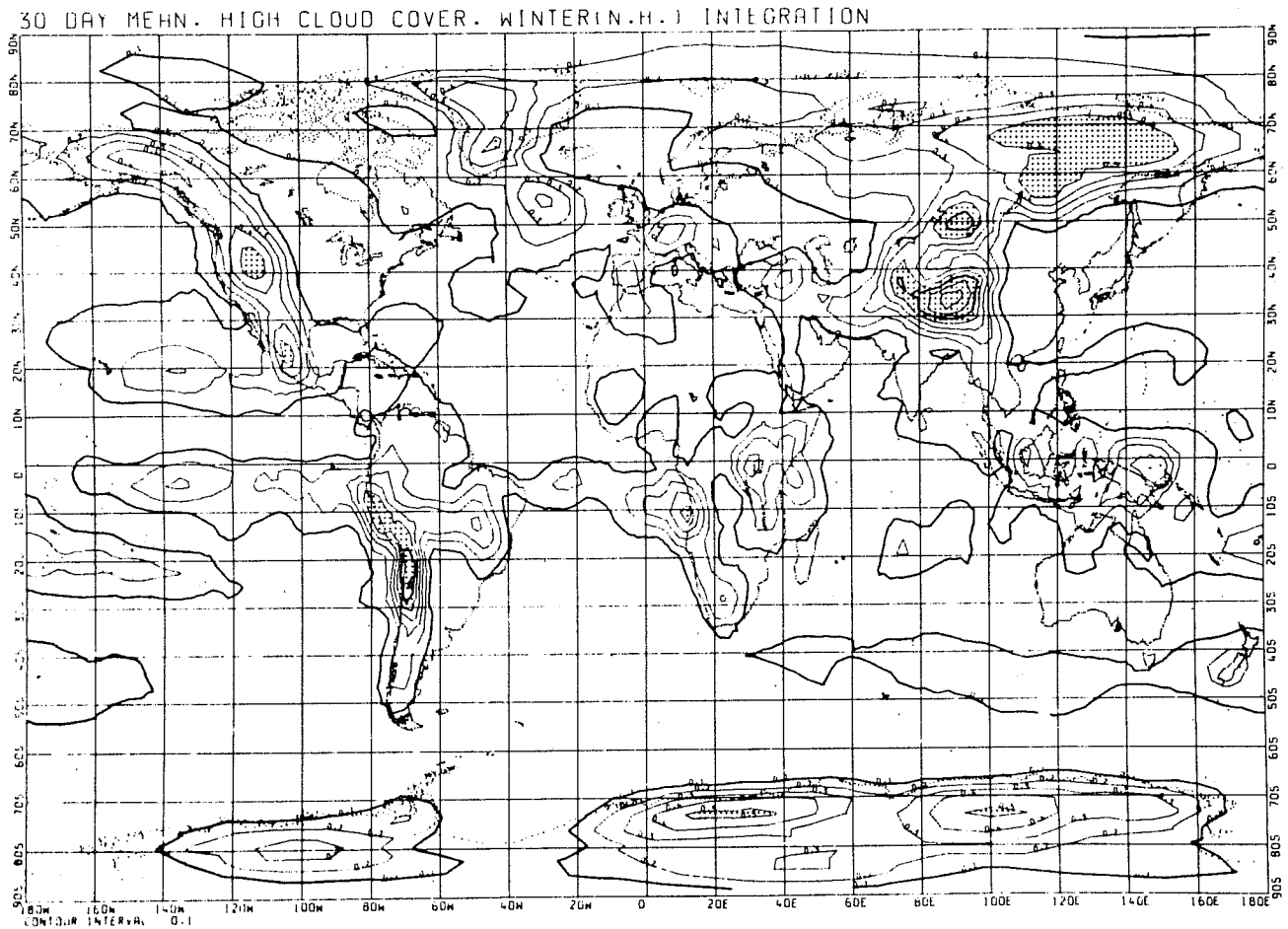

Contour interval = 0.1. Shaded areas have $\geq$ 50% cloud cover.

Fig. 6 30-day mean distribution of high cloud simulated by the model

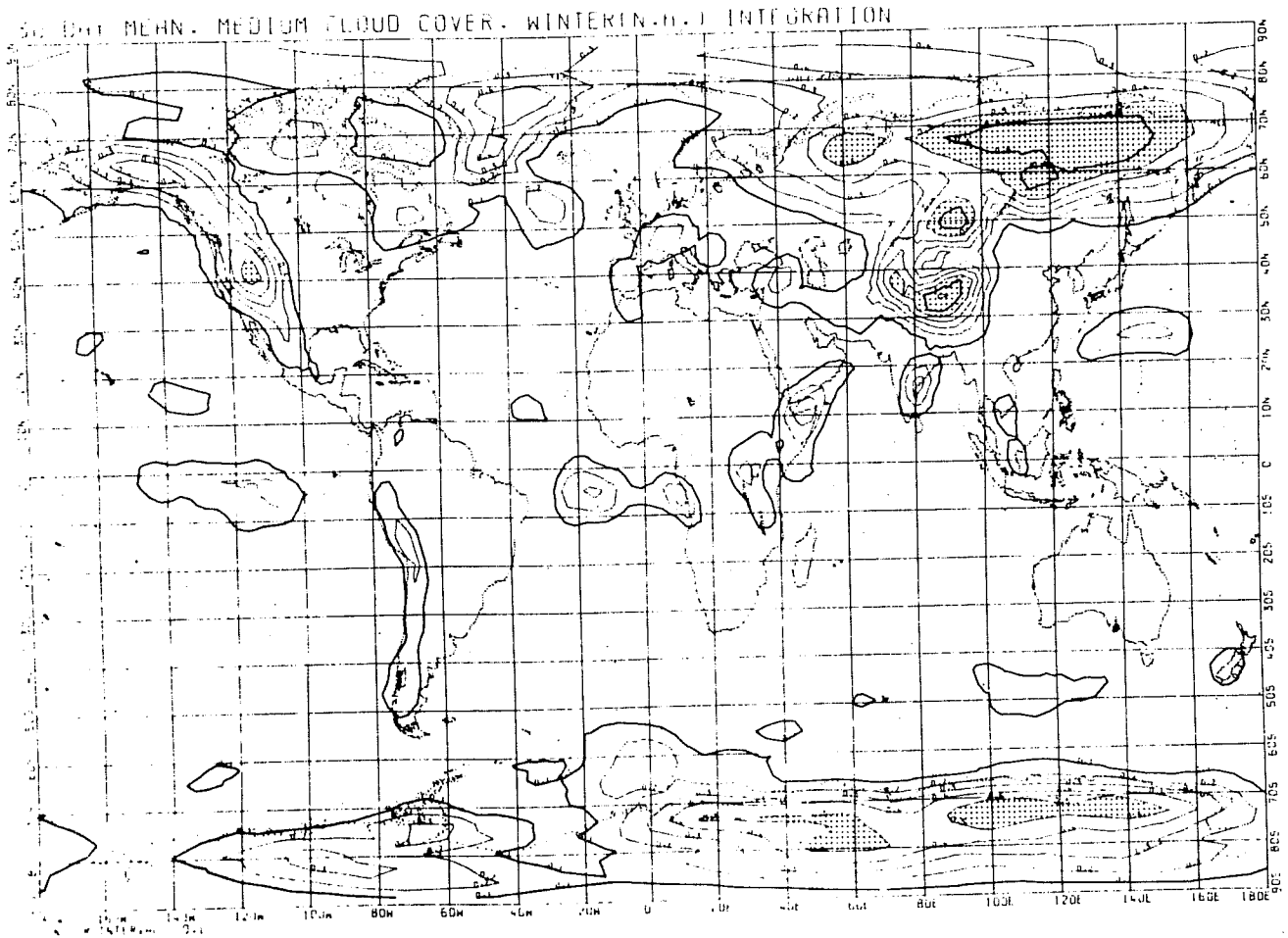

Contour interval = 0.1. Shaded areas have $\geq$ 50% cloud cover.

Fig. 7 30-day mean distribution of medium cloud simulated by the model

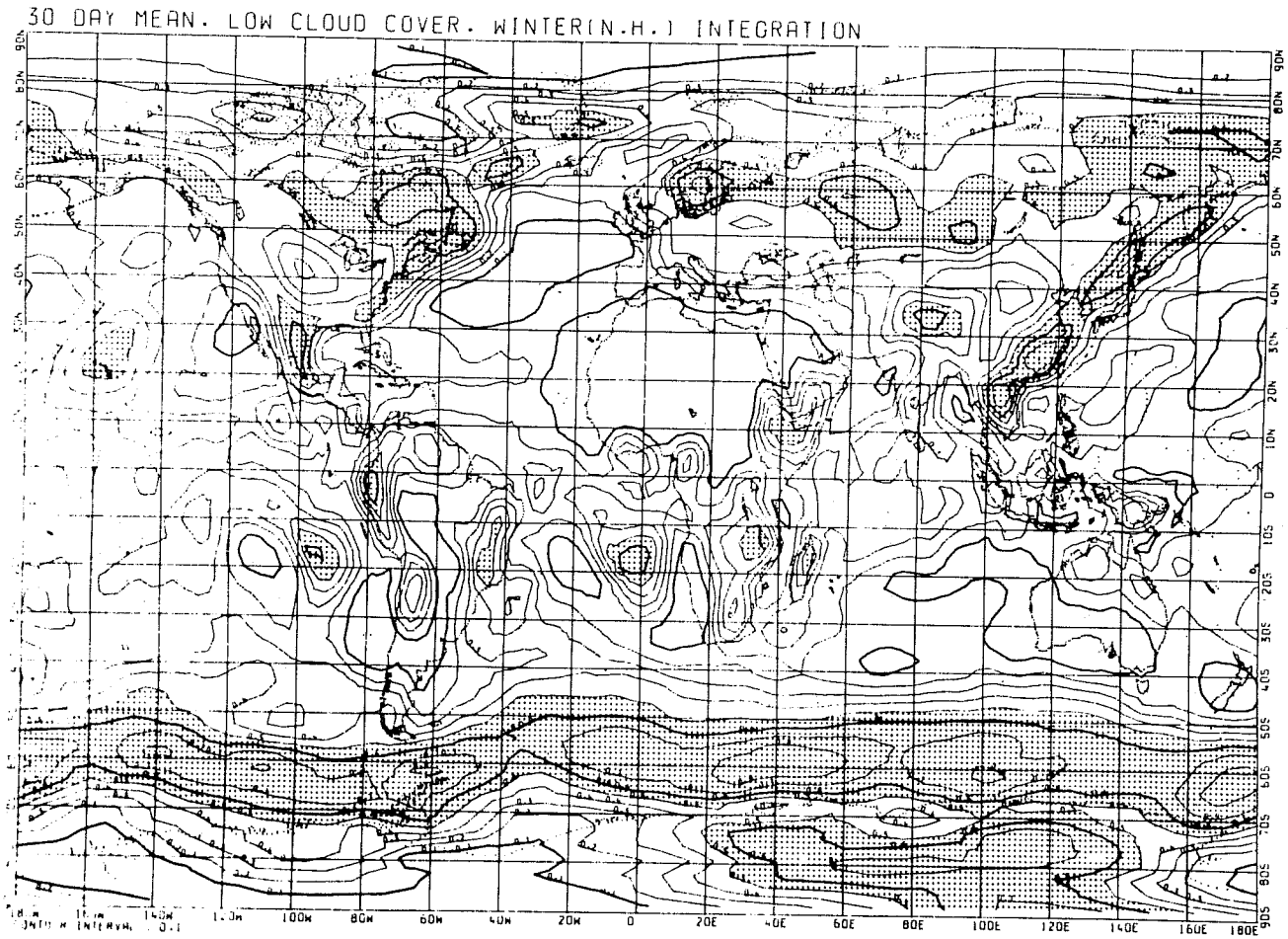

Contour interval = 0.1. Shaded areas have $\geq$ 50% cloud cover.

Fig. 8 30-day mean distribution of low cloud simulated by the model

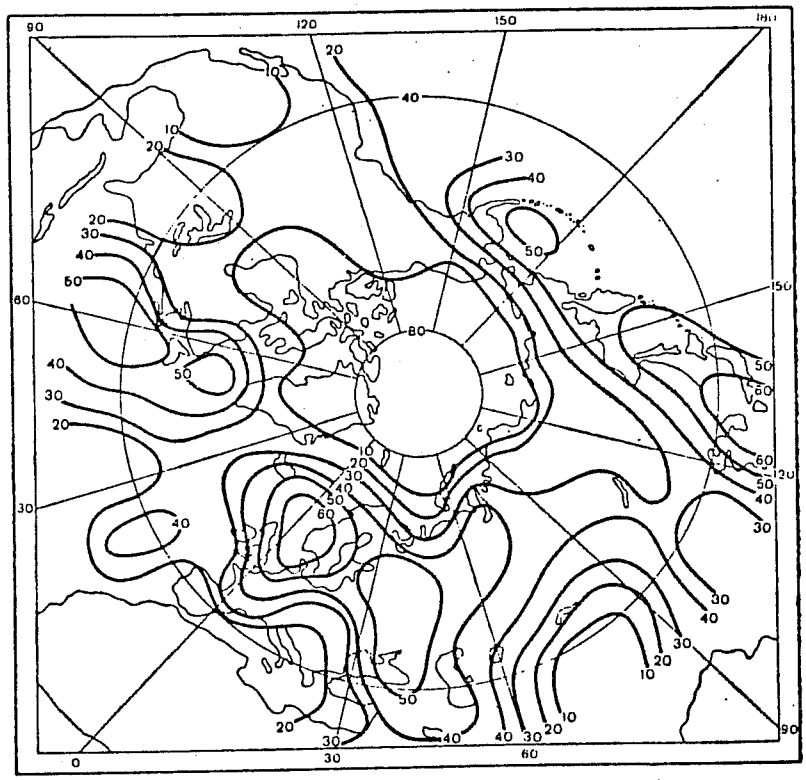

Fig. 9 Observed frequency of occurrence of stratus clouds for January (%) (from Shapovalova 1979)

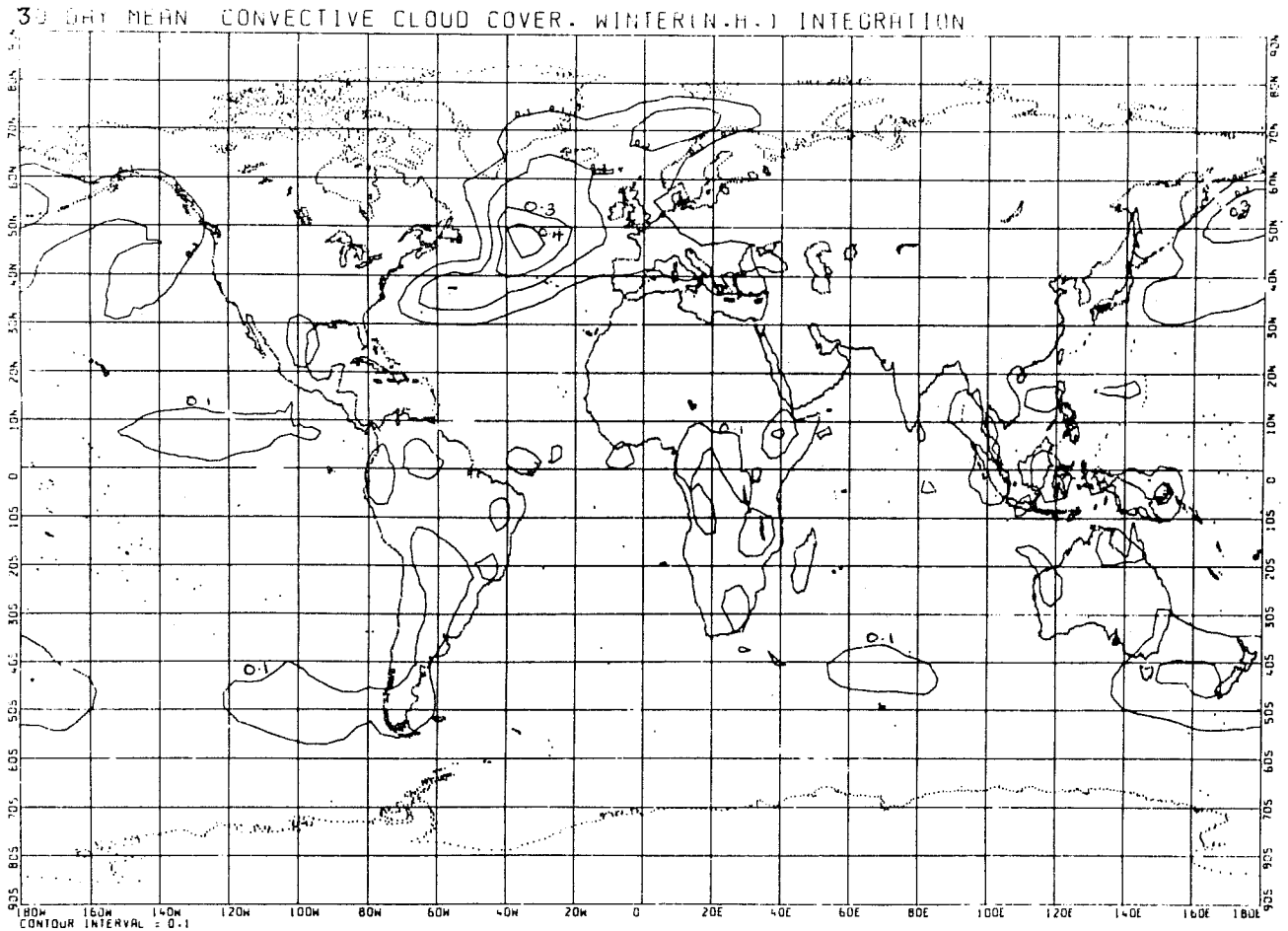

Contour interval = 0.1

Fig. 10 30-day mean distribution of convective cloud simulated by the model

small. This may be due in part to the temporal and spatial variability of the cloud so that a time-meaned field has only small amounts of cloud at any grid point.

A combination of the four cloud fields to give the total cloudiness is shown in Fig. 11 where it can be compared with an observed distribution for January (Fig. 12) taken from 'Understanding Climatic Change, a program for action', US National Academy of Sciences, 1974. In both figures areas of greater than 50% cloudiness have been shaded. The model's distribution agrees reasonably well with the observed distribution. The main discrepancies, such as the excessive cloudiness over the Himalayas and the western United States have already been discussed in the context of the individual cloud fields.

In conclusion, these preliminary results from the cloud parametrization scheme are sufficiently encouraging that further tests of the scheme for different times of the year will be carried out. Certain problems, such as the tendency of the scheme to produce upper level clouds over high topography, need further investigation and it may be necessary to use other model parameters, such as vertical velocity, to overcome these faults.

3. DISCUSSION

A discussion of the effects of fully interactive clouds on the model results has purposely been excluded from this paper. With only one integration completed at this stage, it would be wrong to draw any form conclusions from the results. This is particularly true for the northern hemisphere winter where the model's natural variability is large. More integrations are required before an assessment can be made of the global importance of cloud in the model's performance.

Results from earlier work with the limited area tropical model showed systematic differences between forecasts with and without interactive cloud (Slingo 1978). Over land clouds had a marked effect on convection by controlling the surface fluxes of heat and moisture whereas over the sea, the vertical circulations induced by the horizontal gradients in atmospheric radiative heating enhanced convection both by the greater destabilization occurring in areas of increased ascent and by the greater low-level convergence into the system. The effect of these changes in convective activity led to a greater development of disturbances over the sea during a 3-day forecast. Over land the presence of interactive clouds reduced convection and led to a weakening of the circulation patterns. These results are not unexpected since it is well known that, in tropical latitudes, disturbances are driven primarily by latent heat release from convection which,

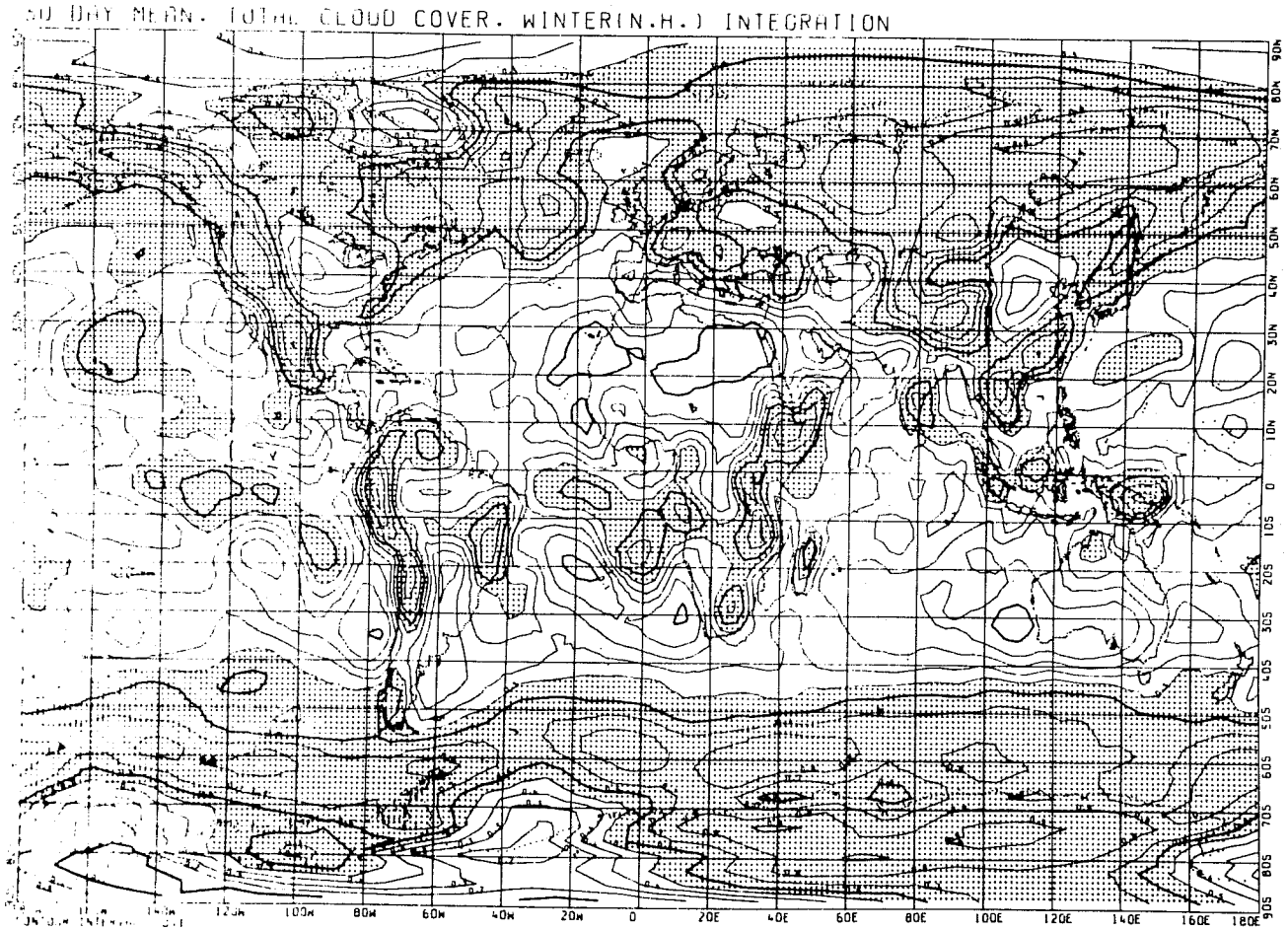

Contour interval = 0.1. Shaded areas have $\geq$ 50% cloud cover.

Fig. 11 30-day mean distribution of total cloudiness simulated by the model

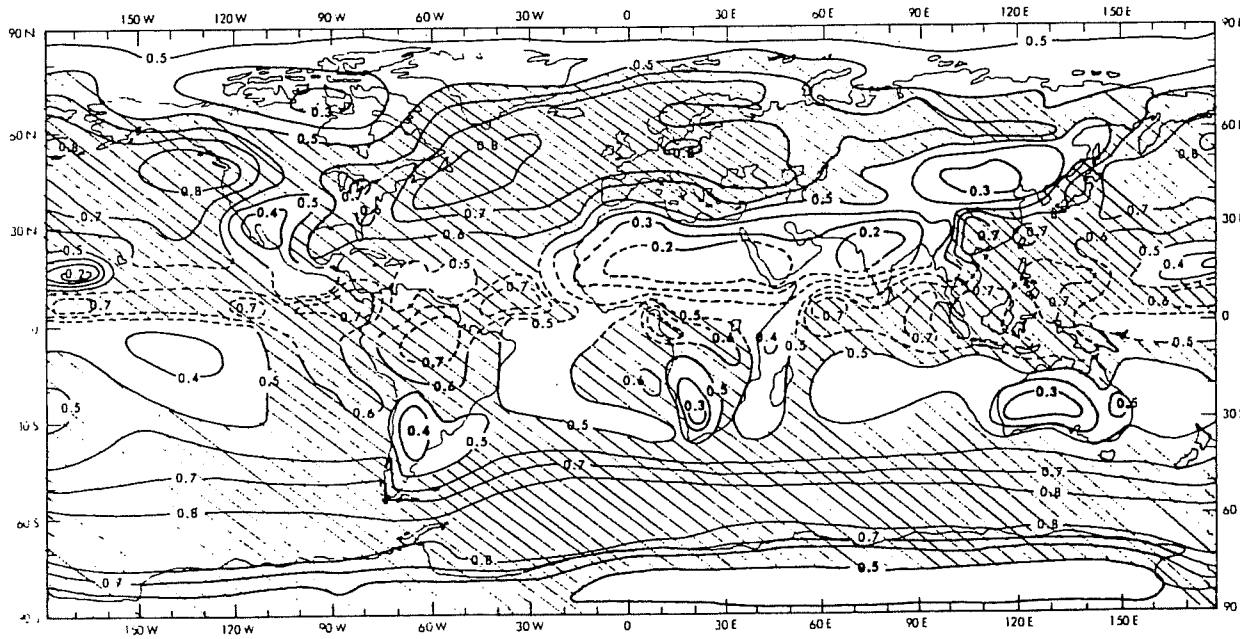

Contour interval = 0.1. Shaded areas have $\geq$ 50% cloud cover.

Fig. 12 Observed distribution of total cloudiness for January from 'Understanding climatic change, a program for action' US National Academy of Sciences, 1974.

in its turn, is sensitive to the radiative cooling profile and the surface heating. The same may not be true for mid-latitude systems since, at this stage, it is unclear how important the various forms of diabatic heating are in the development of a baroclinic wave.

Cloud parametrization schemes, such as that described in this paper, are now fairly successful in predicting realistic cloud distributions. However, one drawback of such schemes is that the prediction of cloud is partially divorced from the rest of the model in that the clouds cannot interact directly with the radiation field that they produce. At present the radiation scheme calculates a net radiative heating rate which is a combination of the heating in the clear air and that in the cloudy air. This final heating rate is then applied to the whole model layer and over the whole grid square. No attempt is made to allow for the fact that in reality the enhanced cooling, say, due to the cloud, acts only in the cloud and in some circumstances is thought to help maintain the cloud rather than have a net cooling effect on the whole system i.e. cloud + environment.

An analogous situation arises in the treatment of convection. Many schemes parametrize convection in terms of an ensemble of buoyant plumes. If saturation occurs as the ensemble ascends then the resultant latent heat release is assigned to the ensemble (not the environment + ensemble). The latent heating enhances the buoyancy of the ensemble so that convection can reach higher levels. The final warming in the model as a result of convection is due to the environmental subsidence and not to latent heat release.

One example where cloud-radiation interaction may be important is in the case of stratocumulus. Detailed observational studies have shown that the radiative effects of the cloud are such as to produce a large cooling in a thin layer at the top of the cloud and a slight warming below. This cooling may have a large effect on the growth of cloud droplets and is thought to play an important part in the energetics of the cloud (Roach et al 1981). In a general circulation model, however, the effect of such a cloud would be parametrized as an enhanced cooling for the whole layer which could then feedback directly into the dynamics. The question is, in reality does the cloud produce a net cooling of the whole layer or does the perturbed heating rate play some direct part in maintaining or dissipating the cloud without having an effect on the large-scale temperature field?

Another example is that of the dense cirrus shields which form in the tropics as a result of outflow from cumulonimbus clouds. When these high clouds are present in the model they give a net radiative warming in the layer which can have a

substantial effect on the model's circulation and rainfall (Slingo 1978). In reality however this warming is not spread evenly through the layer. A recent paper by Webster and Stephens (1980) has shown that there is a thin layer of radiative cooling at the top of the cloud resulting in a large heating differential between the base and top of the cloud. Their study of the extent and longevity of these upper tropospheric clouds during Winter MONEX has led them to suggest that these radiative effects may play an important part in maintaining these clouds. Thus apart from the problem of deriving a cloud distribution from the model fields, the direct interaction of these clouds with the radiative fluxes needs further consideration.

References

Cess, R.D. 1976 'Climate change: an appraisal of atmospheric feedback mechanisms employing zonal climatology', J. Atm. Sci., 33, pp. 1831-1843.

Corby, G.A., Gilchrist, A., and Rowntree, P.R. 1977 'United Kingdom Meteorological Office 5-level general circulation model', Methods in Computational Physics, Academic Press Inc., New York, Vol. 17, pp. 67-110.

Dopplick, T.G. 1970 'Global radiative heating of the earth's atmosphere', Planetary Circulations Project, M.I.T., Cambridge, Report No. 24.

Ellis, J.S., and Vonder Haar, T.H. 1976 'Zonal average earth radiation budget measurements from satellites for climate studies', Atmos. Sci. Paper 240, Colorado State Univ., Fort Collins, Colorado.

Gruber, A. 1978 'Determination of the earth-atmosphere radiation budget from NOAA satellite data', NOAA Tech. Report NESS 76.

Herman, G.F. 1980 'Cloud-radiation experiments conducted with GLAS general circulation models', Proceedings of Workshop on 'Radiation and cloud-radiation interaction in numerical modelling', ECMWF, 15-17 Oct. 1980.

Hunt, G.E. 1976 'A January climatology, zonal heat balance and cloudiness simulated by a Meteorological Office 5-level general circulation model', Met O 20 Tech. Note II/63, Meteorological Office, Bracknell, England.

Hunt, G.E., and Mattingly, S.R. 1976 'Infrared radiative transfer in planetary atmospheres - I: Effects of computational and spectroscopic economies on thermal heating/cooling rates', J. Quant. Spect. Rad. Transfer, 16, pp. 505-520.

Huschke, R.E. 1969 'Arctic cloud statistics from 'air calibrated' surface weather observations', RAND Corp. Memo RM-6173-PR.

Jacobowitz, H. and Others. 1979 'The first 18 months of planetary radiation budget measurements from the Nimbus 6 ERB Experiment', J. Atm. Sci., 36, pp. 501-507.

Kasahara, A., and Washington, W.M. 1971 'General circulation experiments with a six-layer NCAR model, including orography, cloudiness and surface temperature calculations', J. Atm. Sci., 28, pp. 657-701.

London, J., and Others. 1976 'Atlas of the global distribution of total ozone, July 1957-June 1967', NCAR Tech. Note NCAR/TN/113+STR, Boulder, Colorado.

McClatchey, R.A., and Others. 1973 'AFCRL Atmospheric line parameters compilation', Env. Res. Paper No. 434, Air Force Cambridge Research Labs., AFCRL-TR-73-0096.

Manabe, S., and Möller, F. 1961 'On the radiative equilibrium and heat balance of the atmosphere', Month. Weath. Rev., 89, pp. 503-532.

Manabe, S., and Strickler, R.F. 1964 'Thermal equilibrium of the atmosphere with a convective adjustment', J. Atm, Sci., 21, pp. 361-385.

Phillpot, H.R. 1968 'A study of the synoptic climatology of the Antarctic', Melbourne Inst. Antarc. Met. Research Centre, Tech. Report No. 12.

Raschke, E., and Others. 1973 'The radiation balance of the earth-atmosphere system during 1969-70 from Nimbus 3 measurements', J. Atm. Sci., 30, pp. 341-364.

Roach, W.T. 1961 'The absorption of solar radiation by water vapour and carbon dioxide in a cloudless atmosphere', Q. J. R. M. S., 87, pp. 364-373.

Roach, W.T., and Others. 1981 'A field study of nocturnal stratocumulus - I: observations and budgets', Submitted to Q. J. R. M. S.

Sasamori, T., London, J., and Hoyt, D.V. 1972 'Radiation budget of the southern hemisphere', Met. Monographs, Vol. 13, No. 35.

Shapovalova, V.D. 1979 'The distribution of the prevailing forms of cloud cover in the extra-tropical latitudes of the northern hemisphere', T. Vyp. 425, pp. 51-57, Glav. Geof. Obs., Leningrad.

Slingo, Julia 1978 'The effect of interactive clouds and radiation on convective activity in a numerical model of the tropics', Met O 20 Tech. NoteII/130, Meteorological Office, Bracknell, England.

1980a 'A cloud parametrization scheme derived from GATE data for use with a numerical model', Q. J. R. M. S., 106, pp. 747-770.

1980b 'A study of the earth's radiation budget using a general circulation model', Submitted to Q. J. R. M. S.

Telegadas, K., and London, J. 1954 'A physical model of the northern hemisphere troposphere, for winter and summer', New York Univ. Sci. Report No. 1, Contract No. AF 19(122)-165.

US National Academy of Sciences 1974 'Understanding climatic change, a program for action'.

Webster, P.J., and Stephens, G.L. 1980 'Tropical upper-tropospheric extended clouds: Inferences from Winter MONEX', J. Atm. Sci., 37, pp. 1521-1541.

Wilderspin, R. 1980 'Interactive cloud and radiation in the 11-layer model Part III: Extension of the tropical model cloud scheme to the whole globe using FGGE data', Met O 20 Technical Note in preparation.

Winston, J.S. et al. 1979 Earth-Atmosphere Radiation Budget Analyses derived from NOAA Satellite data. June 1974-February 1978, Vol. 1.